

Marrow-Derived Cells Regulate the Development of Early Diabetic Retinopathy and Tactile Allodynia in Mice

Guangyuan Li,^{1,2} Alexander A. Veenstra,¹ Ramaprasad R. Talahalli,¹ Xiaoqi Wang,¹ Rose A. Gubitosi-Klug,¹ Nader Sheibani,³ and Timothy S. Kern^{1,4}

The hypothesis that marrow-derived cells, and specifically proinflammatory proteins in those cells, play a critical role in the development of diabetes-induced retinopathy and tactile allodynia was investigated. Abnormalities characteristic of the early stages of retinopathy and allodynia were measured in chimeric mice lacking inducible nitric oxide synthase (iNOS) or poly(ADP-ribose) polymerase (PARP1) in only their marrow-derived cells. Diabetes-induced capillary degeneration, proinflammatory changes, and superoxide production in the retina and allodynia were inhibited in diabetic animals in which iNOS or PARP1 was deleted from bone marrow cells only. Of the various marrow cells, neutrophils (and monocytes) play a major role in retinopathy development, because retinal capillary degeneration likewise was significantly inhibited in diabetic mice lacking the receptor for granulocyte colony-stimulating factor in their marrow-derived cells. Immunodepletion of neutrophils or monocytes inhibited the endothelial death otherwise observed when coculturing leukocytes from wild-type diabetic animals with retinal endothelium. iNOS and PARP1 are known to play a role in inflammatory processes, and we conclude that proinflammatory processes within marrow-derived cells play a central role in the development of diabetes complications in the retina and nerve. *Diabetes* 61:3294–3303, 2012

Diabetic retinopathy (DR) and neuropathy are leading causes of blindness and pain in industrialized nations. The early stages of DR are characterized by vascular abnormalities (permeability, nonperfusion, and degeneration) and degeneration of some retinal neurons (1,2). The progressive degeneration of retinal capillaries in diabetes can cause retinal ischemia, which then stimulates the subsequent neovascular response characteristic of advanced DR (3,4). Inflammatory markers are also increased in retinas from diabetic patients and animals, and our previous studies have shown that systemic inhibition of inflammation using germline deletion of inducible nitric oxide synthase (iNOS) or an inhibitor of poly(ADP-ribose) polymerase (PARP1) significantly inhibited the capillary degeneration and other early lesions of DR in animals (4–6).

Both iNOS and PARP1 are important proteins in inflammation and immunity (7,8). iNOS is the primary source of nitric oxide (NO) in activated leukocytes, and NO is involved in subsequent modification of protein function (such as nitration or nitrosylation) and enhanced generation of reactive species (including superoxide and reactive nitrogen species) (9–11). PARP1 is a nuclear enzyme that ADP-ribosylates proteins and has important roles in both DNA repair and nuclear factor- κ B-mediated transcription of proinflammatory genes (12,13).

Most studies to date have focused on cells of the retina and its vasculature as the main sites for the biochemical abnormalities that cause diabetes-induced retinopathy. Leukocytes become abnormal in diabetes and adhere to and occlude some blood vessels (14,15). Moreover, whole-body deletion of intercellular adhesion molecule-1 (ICAM-1) or CD18 inhibited development of early DR (16). How this effect was mediated, and whether this finding implicated only marrow-derived cells in the development of the retinopathy, remained unclear. To directly test the contribution of inflammation (specifically proinflammatory processes within myeloid-derived cells) in development of the early stages of DR, we generated chimeric mice that lacked either iNOS or PARP1 only in their marrow-derived cells.

Some diabetic patients develop a hypersensitivity to light touch (tactile allodynia) that can result in pain and discomfort (17). Germline deletion of iNOS or PARP1 or treatment with PARP1 inhibitor significantly inhibits diabetes-induced tactile allodynia (18,19). Microglia (marrow-derived cells) in the spinal cord have been implicated in diabetes-induced allodynia in mice (20). Therefore, we used chimeric animals in which iNOS and PARP1 had been deleted from marrow-derived cells to study the role of leukocytes also in the development of a diabetes-induced neural complication.

RESEARCH DESIGN AND METHODS

Animals. Experiments conformed to the guidelines of the Association for Research in Vision and Ophthalmology (ARVO) and Case Western Reserve University (CWRU). Offspring from breeder pairs of wild type (WT; C57Bl/6J), iNOS^{-/-} (B6.129P2-Nos2^{tm1Lau/J}), GFP (C57Bl/6-Tg[ACTB-EGFP]10sb/J), and PARP1^{-/-} (129S-Parp1^{tm1Zqw/J}) (The Jackson Laboratory) were housed in air-filtered units. Diabetes was induced in male mice with streptozotocin (55 mg/kg) and maintained with 0.1–0.2 units of NPH insulin (0.0217 ± 0.0037 units/g/week/mouse) (6,21,22). Hyperglycemia was quantified via blood glucose concentrations, and every 2–3 months by glycated hemoglobin levels (Variant II total GHb Program; Bio-Rad).

Recipient mice (nondiabetic or diabetic for 2 weeks) were irradiated with two 600-rad doses, 3 h apart, and injected intravenously with 3–5 million bone marrow cells from donor mice. Chimeras lacking iNOS, PARP1, or the receptor for granulocyte colony stimulating factor (G-CSFR) only in their marrow-derived cells were generated by transplanting marrow from iNOS^{-/-}, PARP1^{-/-}, or G-CSFR^{-/-} donors into irradiated WT (C57Bl/6J) hosts (identified for example as iNOS^{-/-}→WT; names to the left and right of arrow refer to marrow donor and recipient, respectively). “Reverse” chimeras lacking

From ¹Case Western Reserve University and Case Medical Center, Cleveland, Ohio; ²The Second Hospital of Jilin University, Changchun, Jilin, China; the ³University of Wisconsin, Madison, Wisconsin; and the ⁴Veterans Administration Medical Center Research Service 151, Cleveland, Ohio.

Corresponding author: Timothy S. Kern, tsk@case.edu.
Received 7 September 2011 and accepted 17 June 2012.
DOI: 10.2337/db11-1249

This article contains Supplementary Data online at <http://diabetes.diabetesjournals.org/lookup/suppl/doi:10.2337/db11-1249/-/DC1>.

G.L. and A.A.V. contributed equally to this study.

© 2012 by the American Diabetes Association. Readers may use this article as long as the work is properly cited, the use is educational and not for profit, and the work is not altered. See <http://creativecommons.org/licenses/by-nc-nd/3.0/> for details.

iNOS or PARP1 in all cells except marrow-derived cells were generated by transplanting marrow from WT donors into irradiated iNOS^{-/-} or PARP1^{-/-} hosts (WT→iNOS^{-/-}). To control for irradiation and chimeric procedures, we generated chimeras in which marrow from WT or mice expressing green fluorescent protein (GFP) was transplanted into WT recipients (WT→WT and GFP→WT, respectively), and in some cases the head of the recipient was shielded with lead during irradiation.

Leukostasis. Leukocytes adherent to retinal vessel walls after perfusion were labeled with fluorescein isothiocyanate (FITC)-concanavalin A (Vector) and counted (6,21,22).

Immunohistochemistry. Retinas perfused with concanavalin A were fixed (paraformaldehyde, 0.03% Triton X-100; 4 h), washed (PBS), and blocked (2× PBS, 0.03% Triton X-100, 20% goat serum, 5% BSA) (23). Flat-mounted retina were stained using anti-collagen-IV (Abcam); concanavalin A (Vector); CD45 (Calbiochem); IBA-1 (Wako); GFP (Rockland); Nymph-R14, 7/4 (AbD-Serotech); MHCIIA/IE, CD11b, B220, and CD4/CD8a (eBioscience); PE (Rockland); rabbit (Jackson ImmunoResearch); and rat IgG2b and rat IgG2a (AbD-Serotech).

mRNA and DNA. mRNA was extracted from retina using RNeasyPlus Mini kits (Qiagen). cDNA was generated with SuperScript-III First-Strand System (Invitrogen) followed by RT-qPCR (Applied Biosystems): iNOS-F1, TCT-TTG-ACG-CTC-GGA-ACT-GTA-GCA; iNOS-R1, TAG-GTC-GAT-GCA-CAA-CTG-GGT-GAA; TNF- α -F1, CAT-CTT-CTC-AAA-ATT-CGA-GTG-ACA-A; TNF- α -R1, TGG-GAG-TAG-ACA-AGG-TAC-AAC-CC; COX-2-F1, CAC-AGC-CTA-CCA-AAA-CAG-CCA; COX-2-R1, GCT-CAG-TTG-AAC-GCC-TTT-TGA; 18S-F1, ACT-CAA-CAC-GGG-AAA-CCT-CAC-C; 18S-R1, CCA-GAC-AAA-TGC-CTC-CAC-CAA-C; ICAM-1-F1, GCC-TTG-GTA-GAG-GTG-ACT-GAG; ICAM-1-R1, GAC-CGG-AGC-TGA-AAA-GTT-GTA.

DNA was extracted from blood using DNeasy kit (Qiagen) and amplified with PCR Supermix (Invitrogen): PARP1-F1, CGA-CAT-GGT-GTC-CAA-AAG-TG; PARP1-R1, GGT-GGT-TTT-TCC-CAA-ACC-TT; iNOS-F1, CAG-CTG-GGC-TGT-ACA-AAC-CTT; iNOS-R1, CAT-TGG-AAG-TCA-AGC-GTT-TCG.

Coculture. Mouse retinal endothelial cells (mRECs; generated from Immortomice) (24) were grown in Dulbecco's modified Eagle's medium containing 10% FBS and 5.5 or 25 mmol/L glucose. The medium was changed every other day for 5 days. When mRECs were 80% confluent (500,000 cells), leukocytes (100,000; purified from blood or bone marrow with red blood cell lysis buffer) were added to the mRECs and incubated for 24 h. Leukocytes (bone marrow) in some groups were preincubated with 1 mmol/L α -lipoic acid or 1 μ g anti-Fas ligand (anti-FasL) (BD) for 1 h. After 24 h, mRECs were gently rinsed with PBS to remove leukocytes, incubated with trypsin for 2 min, and washed twice in PBS. The viability of mRECs was measured by trypan blue exclusion with a hemocytometer. Sample identity was masked during counting.

Leukocytes, isolated from EDTA-anticoagulated peripheral blood (red blood cell lysis buffer), were depleted of specific subsets using anti-Ly6G or CD115-PE (eBiosciences) and anti-PE magnetic beads with an Automax system (Miltenyi). Aliquots of the leukocyte preparation before and after immunodepletion were used in the coculture assay described above. Depletion was verified via flow cytometry using anti-B220-450, CD11b-488, CD115-PE, GR1-649, and CD4/CD8a-APC/750 (eBioscience). B220⁺ and CD4/CD8a⁺ cells were excluded from the analysis of GR1⁺ and CD11b⁺ cells.

Superoxide. Leukocytes, mRECs (after coculture with leukocytes), or retinas from perfused mice were incubated in Krebs-HEPES buffer (with 5 or 25 mmol/L glucose) (25 min, 37°C, 5% CO₂). Luminescence was measured 5 min after the addition of 0.5 mmol/L lucigenin, as previously described (6,25). mREC luminescence values were normalized to the value of mREC (high glucose, no leukocytes) controls for each assay.

Histopathology. Degenerate capillaries and pericyte loss ("pericyte ghosts") were quantified in six to eight fields in the midretina (×400 magnification) of fixed, trypsinized retina as previously reported (3,26). Retinal thickness and number of cells in the ganglion cell layer were measured in formalin-fixed, paraffin-embedded eyes sectioned at the optic nerve with light microscopy (6).

iNOS and CD18 expression. Peripheral blood from carbon dioxide-anesthetized mice was fixed (20 min, 2% paraformaldehyde on ice), stained with CD11b-PE, anti-iNOS (M-19/N-20, Santa Cruz), anti-rabbit-488 (Jackson ImmunoResearch), and the antibodies above (except CD115), and analyzed via flow cytometry (27). CD18 surface expression was similarly evaluated using CD18-PE (eBioscience).

Tactile allodynia. Allodynia was measured using previously reported techniques (28,29). Data are reported as the pressure at the 50% paw withdrawal threshold for each animal in response to Von Frey filaments (Stoelting) of logarithmically increasing stiffness.

Statistical analysis. Groups were compared using ANOVA followed by Fisher post hoc test to generate *P* values. Error bars in graphs represent plus or minus one \pm 1 SD. Sample sizes are indicated in the figure legends or in the figure. Due to differences in donor background strains, PARP1^{-/-}→WT and WT→WT chimeras were not compared.

RESULTS

Evaluation of diabetes and chimeric mice. Experimental induction of diabetes using streptozotocin resulted in a statistically significant (*P* < 0.05) elevation of blood glucose (335 \pm 44 vs. 124 \pm 9 mg/dL for nondiabetic controls) and glycated hemoglobin (11.4 \pm 0.7 vs. 2.9 \pm 0.2% for nondiabetic controls). None of the diabetic groups varied significantly from the diabetic controls with respect to these measurements.

Ten weeks after the marrow transplantation, >94% of the white blood cells in the chimeric animals came from the marrow donor, based on PCR measurements of iNOS or PARP1 DNA or counts of GFP-positive cells in GFP→WT animals. There were no significant differences among diabetic groups with regard to hematocrit (41 \pm 0.8%) or circulating white blood cell count (3.6 \pm 0.4 million cells/mL). All chimeras were found to be healthy except for WT→PARP1^{-/-}, which died within 2 months of irradiation. PARP1 is important in DNA repair, and therefore we assume that irradiation of PARP1^{-/-} mice caused severe damage to DNA, resulting in reduced life expectancy.

Molecular processes regulated by iNOS or PARP1 within marrow-derived cells are major causes of the degeneration of retinal capillaries in diabetic mice.

Thirty weeks after the onset of diabetes, retinas from diabetic animals (both nonirradiated WT and WT→WT) developed the expected significant increases in degenerate (acellular) capillaries (3.1- and 2.5-fold above nondiabetic values, respectively) (Fig. 1) and pericyte loss (Supplementary Fig. 1). These abnormalities are characteristic lesions of the early stages of DR (5,14,16,30–34). In contrast to WT and WT→WT diabetic animals, development of degenerate capillaries was significantly inhibited in diabetic iNOS^{-/-}→WT chimeras (reduced to 1.3-fold above nondiabetic). Vascular pathology in diabetic WT→iNOS^{-/-} (reverse) chimeras was similar to the diabetic WT→WT controls (2.2-fold above nondiabetic), indicating that capillary degeneration was more dependent on iNOS in marrow-derived cells than in retina neuroglia. Capillary degeneration in diabetic PARP1^{-/-}→WT animals likewise was only slightly (although significantly; 1.3-fold) greater than the nondiabetic value, suggesting inhibition of diabetes-induced capillary degeneration secondary to deleting PARP1 from leukocytes. This interpretation must be tempered by the recognition that the C57Bl/6 strain is not a perfect control for the 129S strain from which the PARP1 was deleted (see DISCUSSION). No significant differences in retinal capillary loss were found between nondiabetic chimeras or between nondiabetic irradiated and nonirradiated controls, indicating that the irradiation process did not increase capillary loss.

The number of capillary pericyte ghosts was not significantly different between diabetic controls and diabetic chimeras lacking iNOS or PARP-1 (Supplementary Fig. 1); however, an unexplained variability in pericyte loss in some groups of nondiabetic chimeras confounded the ability to assess the effect of diabetes in the various groups.

Thirty weeks of diabetes did not significantly alter either retinal thickness or the number of cells in the ganglion cell layer (Supplementary Table 1) in the WT C57Bl/6 mice, so the effect of diabetes on these parameters in the chimeras was not assessed.

Effect of iNOS and PARP1 on retinal superoxide in diabetes. It has been reported previously (21,25,35) that diabetes results in the increased generation of superoxide

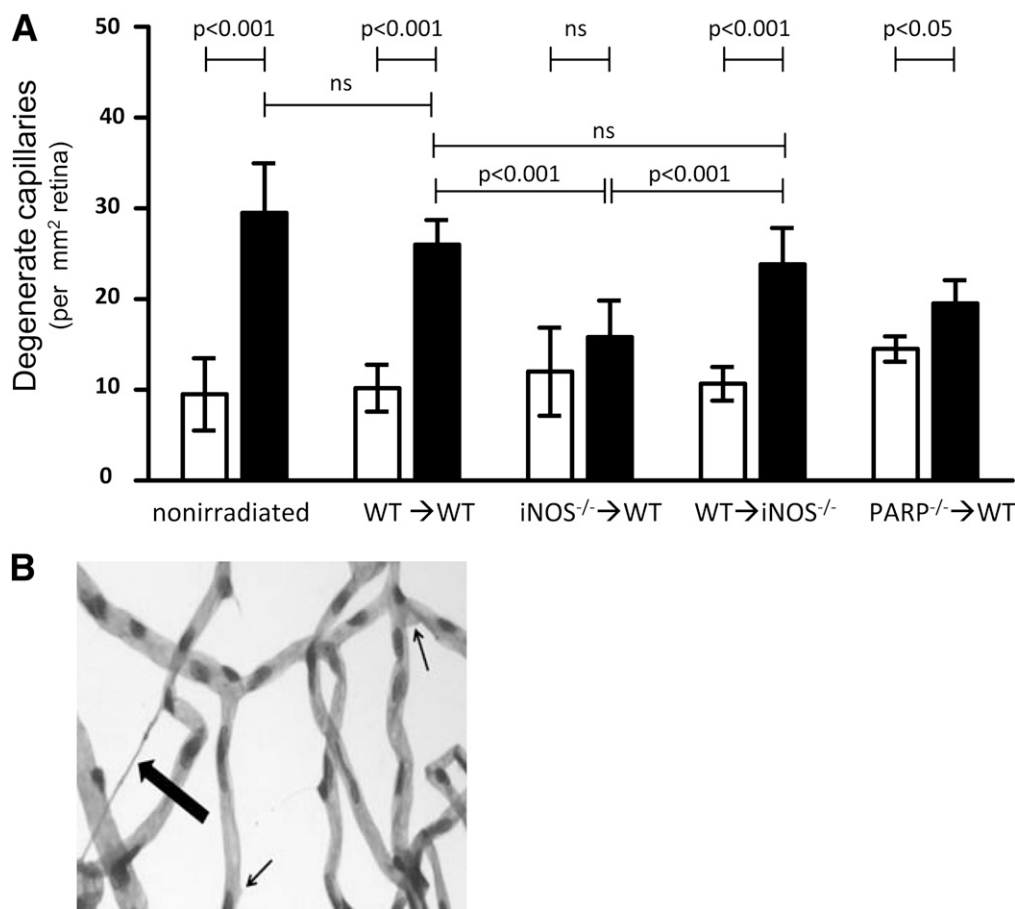


FIG. 1. Diabetes-induced retinal vascular pathology is inhibited in chimeric mice lacking either iNOS (iNOS^{-/-}→WT) or PARP1 (PARP1^{-/-}→WT) in bone marrow-derived cells only. **A:** Degeneration of retinal capillaries is significantly inhibited in iNOS^{-/-}→WT or PARP1^{-/-}→WT mice, but not in “reverse” chimeras (lacking these enzymes throughout the body except marrow-derived cells; WT→iNOS^{-/-}; WT→PARP1^{-/-} was lethal) ($n = 6$). No significant differences in retinal capillary loss were found between nondiabetic chimeras or between nondiabetic irradiated and nonirradiated controls. **B:** Degenerate capillaries (thick arrow) and rare pericyte “ghosts” (thin arrows) in the retinal vasculature. Diabetes duration was 30 weeks. Nondiabetic, white bars; diabetic, black bars ($n > 6$ per group).

by retinas of WT animals, and the ability of therapies to inhibit this increase predicted whether or not the therapy would inhibit diabetes-induced capillary degeneration (6,21,35). To differentiate superoxide generation by retinal cells from that of blood cells in the blood vessels, blood was removed by perfusion in chimeric mice (2 months diabetic). The number of residual leukocytes after perfusion (<20 per retina) is not sufficient to account for the increase in retinal superoxide, because ex vivo measurement of superoxide with 100-fold more leukocytes (isolated from diabetic mice) yielded <1% of the superoxide measured in the retina. The diabetes-induced increase in superoxide generation observed in retinas collected from perfused nonirradiated or WT→WT animals was significantly less in retinas collected from perfused iNOS^{-/-}→WT or PARP1^{-/-}→WT chimeras, but not in WT→iNOS^{-/-} chimeras (Fig. 2A). Similarly, diabetes-induced superoxide production by leukocytes (bone marrow) was significantly increased in WT controls (3.5-fold above nondiabetic value) and in WT→iNOS^{-/-} (3.9-fold) (all $P < 0.05$) but inhibited in iNOS^{-/-}→WT or PARP1^{-/-}→WT chimeras (both 1.2-fold, not significant).

To investigate whether marrow-derived cells from diabetic animals might increase superoxide in capillary cells, mRECs were cocultured with peripheral blood leukocytes from nondiabetic or diabetic mice. mRECs cocultured with

leukocytes from diabetic WT animals generated more superoxide than either mRECs cocultured with leukocytes from nondiabetic WT animals or mRECs grown in either high or low glucose media without leukocytes (Fig. 2B). mRECs incubated with leukocytes from diabetic iNOS^{-/-}→WT animals, in contrast, did not exhibit significant increases in mREC superoxide production compared with mRECs incubated with leukocytes from diabetic WT mice. We conclude that much of the diabetes-induced generation of superoxide measured in isolated retinas required involvement of marrow-derived cells.

Effect of iNOS and PARP1 in marrow-derived cells on diabetes-induced retinal markers of inflammation. mRNA for iNOS, cyclooxygenase-2 (COX-2), tumor necrosis factor- α (TNF- α), and ICAM-1 (Fig. 3A) and leukostasis (Fig. 3B) were significantly increased at 2 months of diabetes in retinas from perfused WT mice, and these increases were significantly inhibited in diabetic iNOS^{-/-}→WT and PARP1^{-/-}→WT chimeras. The diabetes-induced increase in leukostasis was not significantly inhibited in WT→iNOS^{-/-} reverse chimeras, demonstrating that iNOS in marrow-derived cells had more influence on leukostasis than iNOS in cells of the retina. There was a slight, but significant, increase in leukostasis caused by irradiation (nonirradiated, nondiabetic vs. WT→WT nondiabetic animals) (Fig. 3B), which was observed in all nondiabetic

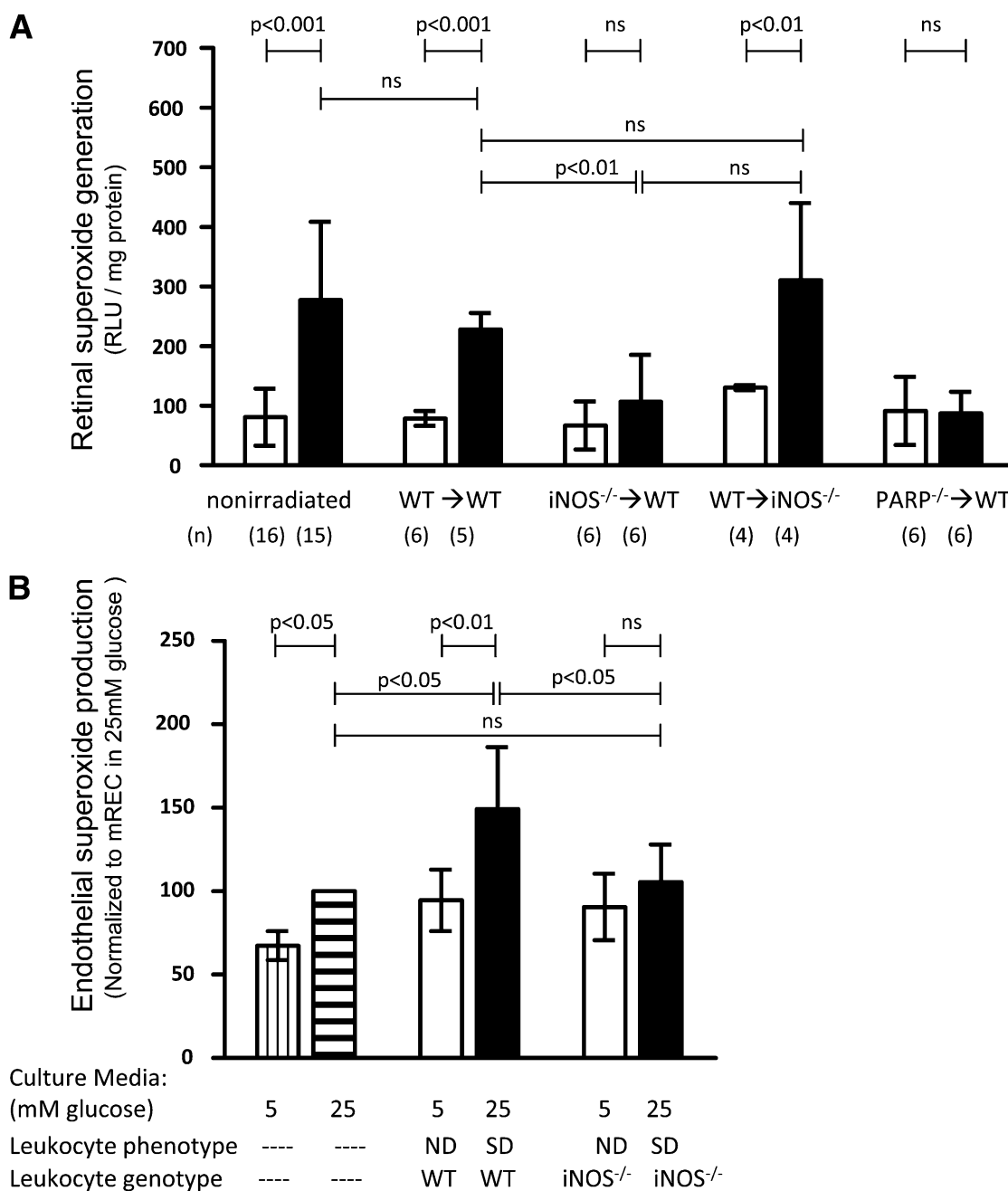


FIG. 2. The diabetes- or glucose-induced increase in superoxide production is significantly inhibited in chimeric mice lacking either iNOS or PARP1 in marrow-derived cells only (iNOS^{-/-}→WT or PARP1^{-/-}→WT) but not in chimeric mice lacking iNOS in all cells except bone marrow (reverse chimera, WT→iNOS^{-/-}). **A:** Retinal superoxide generation. Nondiabetic, white bars; diabetic, black bars. Duration of diabetes was 8–10 weeks. *n* as indicated below the graph. **B:** mRECs cocultured with leukocytes from diabetic animals generated more superoxide than mRECs cocultured with leukocytes from nondiabetic mice or mRECs in high-glucose culture media. This leukocyte-induced enhancement of mREC superoxide generation is inhibited if the leukocytes are isolated from diabetic mice deficient in iNOS. (Data were normalized to superoxide production of mRECs in high glucose, *n* = 5.) mRECs cultured in normal glucose media (no leukocytes), white bars with vertical stripes; mRECs cultured in high glucose media (no leukocytes), white bars with horizontal stripes; mRECs cocultured with leukocytes from nondiabetic mice, white bars; mRECs cocultured with leukocytes from diabetic mice, black bars. Duration of diabetes was 3 months.

chimeras (no significant change in leukostasis between irradiated, nondiabetic chimeras and the nondiabetic WT→WT control). Shielding the head during irradiation did not alter diabetes-induced retinal leukostasis compared with unshielded diabetic animals (Supplementary Fig. 2). Nevertheless, the deletion of iNOS or PARP from marrow-derived cells significantly inhibited diabetes-induced leukostasis compared with the similarly irradiated WT→WT diabetic animals, indicating that the inhibition of diabetes-induced

leukostasis in iNOS- and PARP-deficient leukocytes was not due merely to irradiation.

Leukocyte movement into the retina in diabetes. Having determined that myeloid-derived cells were involved in the pathogenesis of vascular lesions of the retina in diabetes, we next sought to assess if the retina might be damaged by a classical model of leukocyte-mediated infiltration and inflammation. We investigated if cells migrated out of the vasculature into neural retina using

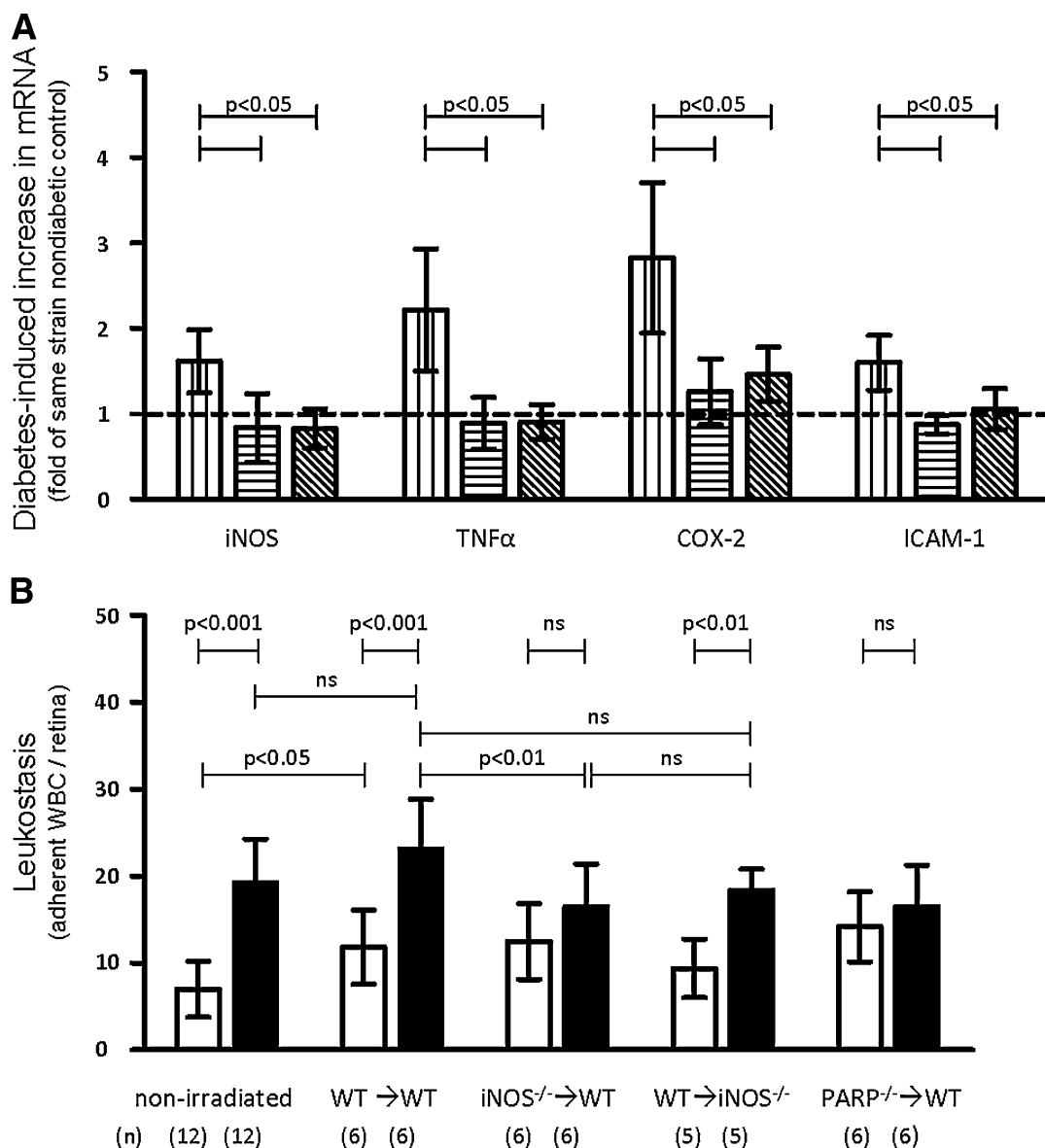


FIG. 3. Diabetes-induced increases of mRNA (for molecules associated with inflammation) and leukostasis are significantly inhibited in chimeric mice lacking iNOS in marrow-derived cells only. **A:** The increase in diabetes-induced retinal mRNAs for iNOS, TNF- α , COX-2, and ICAM-1 is inhibited (compared with nondiabetic controls) in animals lacking iNOS in bone marrow-derived cells only. Diabetic chimeras lacking PARP1^{-/-} likewise are only slightly greater than their nondiabetic controls. WT, white bars with vertical stripes; iNOS^{-/-}→WT, white bars with diagonal stripe; PARP1^{-/-}→WT, white bars with horizontal stripes. Duration of diabetes was 8–10 weeks. $n = 4$ animals per group. All values were normalized to nondiabetic values of each group. Statistical comparisons indicated by horizontal bars lacking P values are all $P < 0.05$. **B:** The diabetes-induced increase in leukocytes adherent to the interior lumen of retinal blood vessels is inhibited in animals lacking either iNOS or PARP1 in bone marrow-derived cells only. No significant differences in leukostasis were observed between nondiabetic chimera groups. Nondiabetic, white bars; diabetic, black bars. (Reverse chimera mice WT→PARP1^{-/-} animals died prior to experiment and thus were not included.) Duration of diabetes was 8–10 weeks. n as indicated below the graph. WBC, white blood cell.

immunohistochemical techniques on flat-mounted retinas from both WT and GFP→WT chimeric mice at 10 and 30 weeks of diabetes. Neither CD45⁺ nor GFP⁺ cells were observed to be part of the vasculature. Outside of the vasculature of diabetic mice, we identified ramified IBA-1⁺ microglia and perivascular macrophages (Supplementary Fig. 3) and a small number of CD45⁺ cells, the majority of which were costained with concanavalin A, suggesting emigration post-profusion. Myeloid-derived microglia are known to migrate into the retina even in nondiabetic animals (36), and our quantification of movement of GFP⁺ microglia into the neural retina indicated that there was no effect of diabetes on the rate that these cells moved

into the retina (Supplementary Fig. 4). The apparent absence of leukocytes in the neural retina of diabetic mice was not due to technical problems, as we were able to detect 7/4⁺/MHCII⁻ (a putative neutrophil population) and 7/4⁺/MHCII⁺ (a putative monocyte population) leukocytes within the lumen of retinal blood vessels. Irradiation diminished the number of IBA-1⁺ microglia in the outer (but not inner) plexiform layer by 42% compared with non-irradiated, diabetic controls, despite having no effect on the severity of diabetes-induced retinal microvascular disease (diabetic WT→WT vs. diabetic, nonirradiated, WT animals) (data not shown). We interpret these data as indicating that it is unlikely that the microglia in the retina

contribute appreciably to the diabetes-induced vascular injury, since a reduction in their number did not similarly reduce vascular pathology. Therefore, the retinal vascular damage in diabetes is likely attributed to the marrow-derived cells remaining within the blood vessels.

Mechanism of leukocyte-mediated retinal injury in diabetes. To investigate how capillary cells might be injured by marrow-derived cells from diabetic animals, mRECs were incubated with purified leukocytes (from bone marrow) from nondiabetic or diabetic mice. After 24-h coculture, the number of dead mRECs was significantly increased by leukocytes from WT diabetic mice compared with nondiabetic WT mice (independent of whether the endothelial cells had been incubated in 5 or 30 mmol/L glucose) (Fig. 4). Since leukocytes might damage vascular endothelium via direct contact (such as via the Fas/FasL system) (37,38) or release of soluble mediators such as superoxide (39), we examined both possibilities. The increase in endothelial death during cocubation with leukocytes from diabetic animals was significantly inhibited by addition of the antioxidant lipoic acid or a blocking antibody against FasL during the incubation. Coculture of mRECs with leukocytes from diabetic animals lacking iNOS resulted in fewer dead endothelial cells than did leukocytes from WT diabetic animals, and neither lipoic acid nor anti-FasL treatment had any additional benefit with iNOS^{-/-} leukocytes. We conclude that marrow-derived cells in diabetes can kill endothelial cells by release of soluble factors as well as contact-mediated routes, and deletion of iNOS from leukocytes inhibits this process.

Since leukocyte-mediated death of mRECs was reduced in the absence of iNOS, we determined which subsets of peripheral blood leukocytes upregulate iNOS in diabetes. Flow cytometry demonstrated that $4.02 \pm 2.35\%$ of neutrophils (GR-1^{high}, CD11b⁺, b220⁻, CD4⁻, and CD8a⁻) and $3.46 \pm 2.67\%$ of monocytes (GR-1^{low}, CD11b⁺, b220⁻, CD4⁻, and CD8a⁻) had elevated levels of iNOS in blood from mice diabetic for 3 months, compared with 0.66 ± 0.47 and $0.58 \pm 0.64\%$, respectively, in nondiabetic mice ($P < 0.015$ and 0.05) (Supplementary Fig. 5). Thus, iNOS-mediated death of retinal endothelial cells is caused by only a small subset of leukocytes.

Evaluation of leukocyte subpopulations on vasculature damage in diabetes. To determine which subpopulation of marrow-derived cells was contributing to endothelial death, Ly6G⁺ or CD115⁺ leukocytes were removed by immunodepletion from the peripheral blood of WT diabetic and nondiabetic mice (40), and removal was confirmed by flow cytometry (Supplementary Figure S6 and Table 2). Ly6G and CD115 are regarded as markers of cells from granulocyte and monocytes lineages, respectively. Depletion of either Ly6G⁺ or CD115⁺ cells from the leukocytes of diabetic animals reduced endothelial death in coculture experiments by 44 ± 11 and $50 \pm 15\%$, respectively (Fig. 5A), compared with a non-immunodepleted aliquot of the same sample. These data are consistent with an interpretation that both neutrophils and monocytes contribute to endothelial death in these cocultures, but since the CD115 immunodepletion also depleted some granulocytes (Supplementary Table 1), the role of monocytes

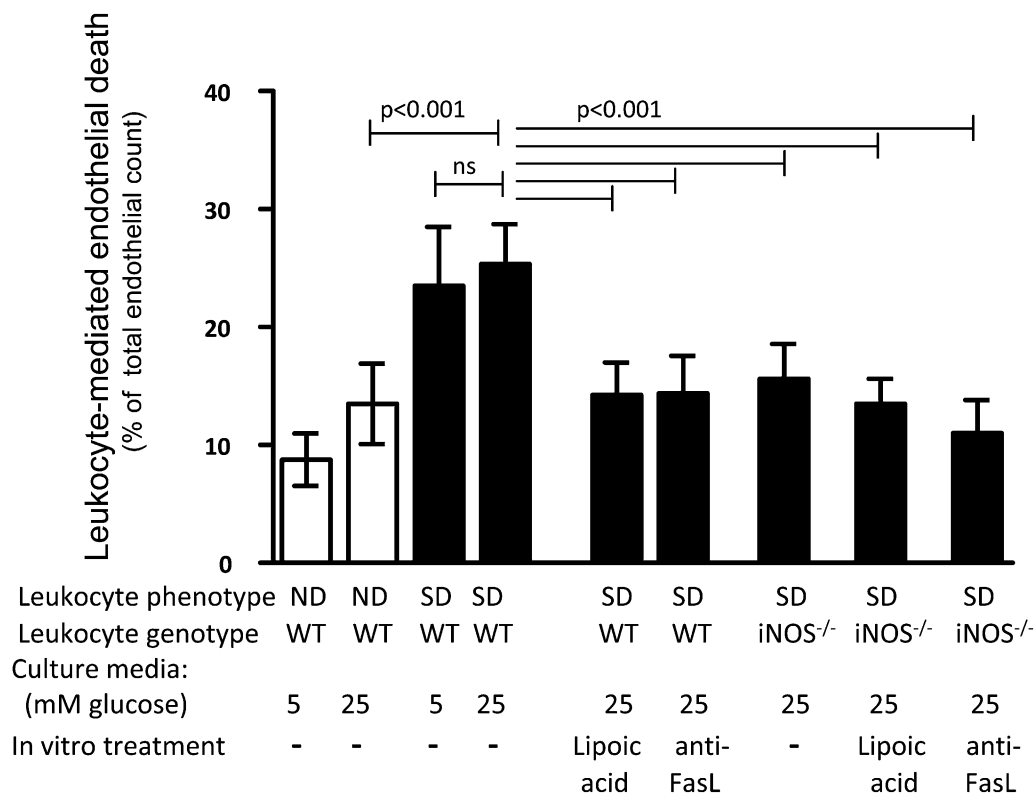


FIG. 4. Diabetes enhances the ability of leukocytes to kill mRECs in vitro. Leukocytes from diabetic WT animals cocultured with mRECs caused more cell death than leukocytes from nondiabetic WT mice, and this effect was independent of the glucose concentration (high or normal) in the culture media. Leukocyte-mediated mREC death was inhibited by lipoic acid (1 mmol/L) or a blocking antibody against FasL (1.0 μ g/mL) in the cocultures, or by using leukocytes lacking iNOS. mRECs cocultured with leukocytes from nondiabetic mice, white bars; mRECs cocultured with leukocytes from diabetic mice, black bars. $n = 4$. Statistical comparisons indicated by horizontal bars lacking P values are all $P < 0.001$.

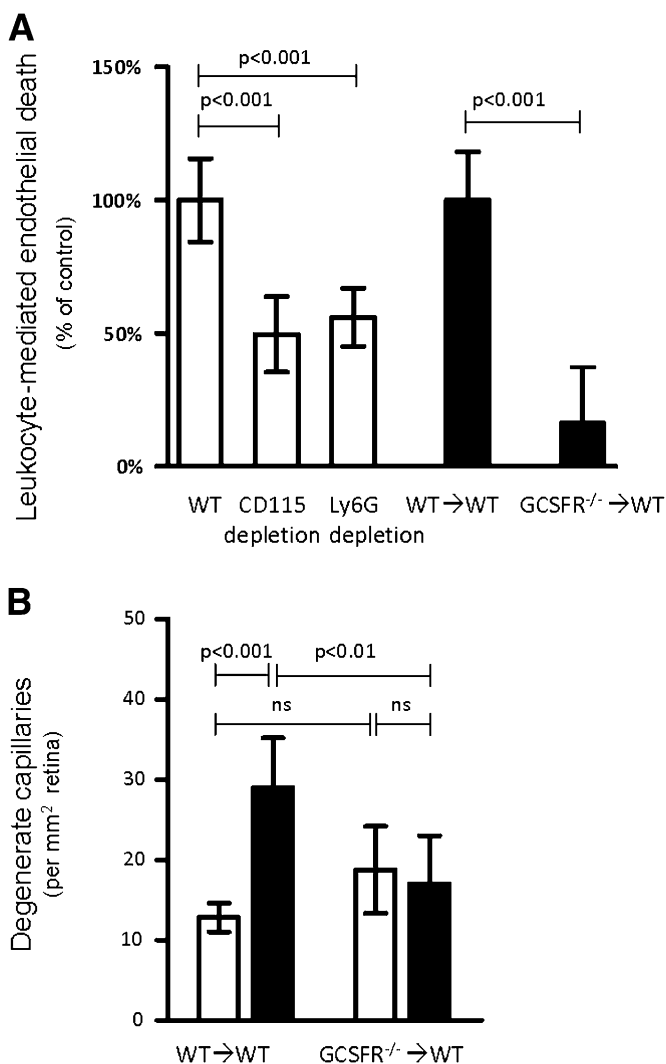


FIG. 5. Neutrophils are a major contributor to endothelial death and vascular degeneration in diabetes. **A:** In vitro killing of mRECs by leukocytes isolated from WT diabetic mice was significantly reduced when the leukocytes were immunodepleted of Ly6G⁺ or CD115⁺ cells (white bars; $n = 8$), or when leukocytes were isolated from diabetic G-CSFR^{-/-} → WT chimeras (not immunodepleted) (black bars; $n = 3$). The diabetes-induced increase in endothelial death due to incubation with leukocytes from each experimental group (i) was set to 100% by the formula $(SD_i - ND_i) / (Avg[SD_{WT}] - Avg[ND_{WT}])$. **B:** Chimeric mice lacking the receptor for G-CSFR in marrow-derived cells were protected from diabetes-induced degeneration of retinal capillaries (30 weeks duration of diabetes; $n = 4$). White bars, nondiabetic; black bars, diabetic.

in endothelial death cannot be unequivocally established from this data.

The causal role of neutrophils in the vascular histopathology of DR was confirmed in long-term in vivo experiments. G-CSF controls maturation of myeloid precursor cells into granulocytes, and severe neutropenia develops in its absence (41). Chimeric mice that lacked receptor for G-CSFR only in their marrow-derived cells (G-CSFR^{-/-} → WT) were generated, and effects on diabetes-induced degeneration of retinal capillaries were assessed at 10 months of diabetes. Granulocytes were reduced from 18 to 1.6% in the G-CSFR^{-/-} → WT chimeras (Supplementary Fig. 6 and Table 2). Diabetes-induced capillary degeneration was significantly inhibited in G-CSFR^{-/-} → WT chimeras (Fig. 5B). Coculture of leukocytes from diabetic G-CSFR^{-/-} animals

with mRECs likewise resulted in significantly less endothelial death than that detected after incubation with leukocytes from WT diabetic animals (Fig. 5A). Efforts to generate chimeras in which marrow cells were deficient in MCSF-R (deficient in cells of the monocyte lineage) (42) were not successful in long-term studies, because monocytes (CD115⁺, CD11b⁺, and GR-1^{low} cells) unexpectedly repopulated the marrow in diabetic animals but not in nondiabetic controls (not shown).

Effect of iNOS and PARP1 on tactile allodynia. As reported previously (28,43), WT diabetic rodents develop a hypersensitivity to light touch compared with nondiabetic controls. We show that proinflammatory processes in leukocytes are required for the development of diabetes-induced tactile allodynia. Tactile allodynia developed in both naive WT and WT → WT diabetic animals but not in diabetic iNOS^{-/-} → WT or PARP1^{-/-} → WT chimeras (Fig. 6). Thus, myeloid-derived cells are major contributors to the dysfunction of peripheral tactile allodynia in diabetic mice, and these processes are regulated at least in part by iNOS or PARP1 within the myeloid cells.

DISCUSSION

Our current results demonstrate that molecular processes regulated by iNOS or PARP1 in bone marrow-derived cells are critical to the development of diabetes-induced retinopathy and allodynia. Since iNOS and PARP1 both have proinflammatory actions in diabetes and other diseases (4,44,45), the current study suggests that proinflammatory processes in marrow-derived cells play critical roles in the capillary degeneration and other lesions of the early stages of DR and allodynia.

Although marrow from iNOS^{-/-} animals was transplanted into the recommended background strain, the PARP1^{-/-} bone marrow was obtained from mice derived on a 129S background, so we cannot exclude the possibility that the presence of 129S marrow in a C57Bl/6 host inhibited by a different mechanism the diabetes-induced retinal inflammation otherwise observed in WT → WT diabetic animals. Nevertheless, both 129S and C57Bl/6 are MHC b haplotype, and neither have any known immunodeficiencies that would confound interpretation of histopathology in the current study. The systemic inhibition of PARP1 with PJ34 (5) has been shown to inhibit diabetes-induced retinal inflammatory-like processes and vascular loss, so we conclude that beneficial effects reported herein for PARP1^{-/-} → WT chimeras are most likely due to the lack of PARP1, and not a genetic difference between C57Bl/6 and 129S strains.

Oxidative stress has been implicated in the development of DR (21,25,35), and systemic inhibition of that stress has inhibited the early stages of DR (6,21,35). Although several different types of cells found in the retina have been found to produce increased superoxide in hyperglycemia or diabetes, we demonstrate that the coculture of leukocytes from diabetic animals with mRECs results in a significantly higher superoxide output from mRECs than that observed due to high glucose media alone (no leukocytes), leukocytes from nondiabetic animals, or leukocytes from iNOS^{-/-} → WT diabetic animals. White blood cells are known to provide products to retinal endothelial cells by transcellular delivery (46), resulting in production of proinflammatory/toxic products by retinal cells (which we speculate includes superoxide).

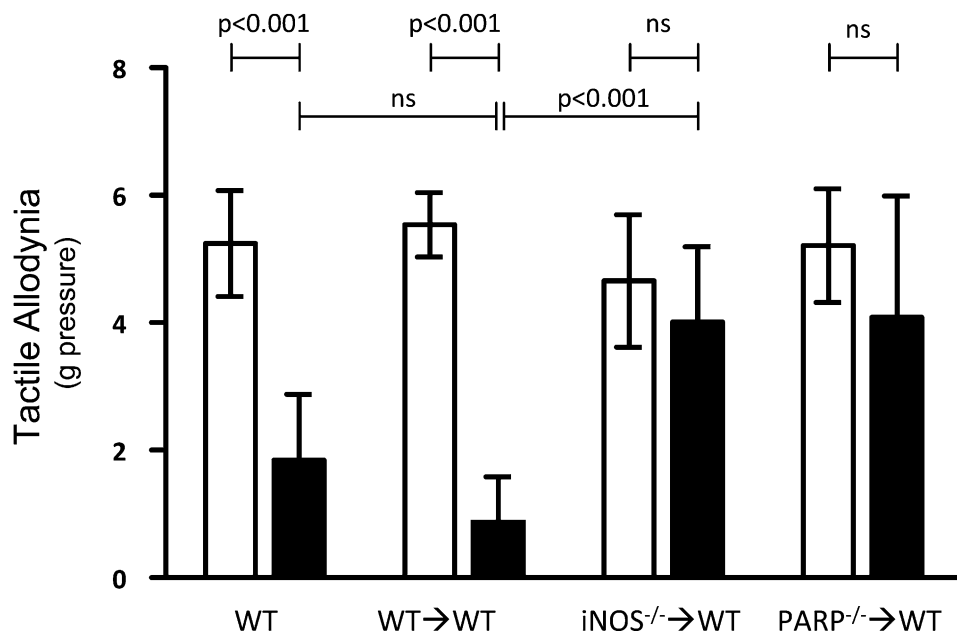


FIG. 6. Pressure on the hind paw required to elicit a response (tactile allodynia) is altered in diabetic mice, and this effect was inhibited in chimeric mice lacking either iNOS or PARP1 in bone marrow-derived cells only. Reported as the pressure threshold at which the paw is withdrawn 50% of the time. White bars, nondiabetic; black bars, diabetic. $n \geq 6$ animals per group.

We did not observe an effect of diabetes (at 10 or 30 weeks duration) on leukocyte emigration into the neural retina. Whether emigration occurs earlier in diabetes is unclear. We speculate that classical transmigration of leukocytes from the vasculature into the neural retina is not a necessary part of the mechanism by which leukocytes mediate diabetes-induced degeneration of capillaries.

Adherence of leukocytes to the luminal walls of the retinal vasculature clearly is increased in diabetes unless either iNOS or PARP1 is absent from marrow-derived cells, but it has not been clear what role, if any, adherence might play with respect to damage of the retinal tissue. Leukostasis might contribute to retinal damage through vessel occlusion resulting in hypoxia, activation of endothelial cells through ICAM-1 dimerization, or simply as a tether during transcellular substrate delivery. However, some reports (35,47) have dissociated leukostasis from diabetes-induced degeneration of retinal capillaries.

Leukostasis requires “activation” of leukocytes and endothelial cells. It has been previously reported that iNOS^{-/-} leukocytes challenged with lipopolysaccharide exhibit increased binding (48). Our studies show that CD18 is expressed on the surface of leukocytes in the iNOS^{-/-} chimeras (Supplementary Table 3). Diabetes-induced increase in ICAM-1 mRNA (marker of endothelial activation) is inhibited in retinas of iNOS^{-/-}→WT or PARP-1^{-/-}→WT chimeras (Fig. 3A). Similarly, the diabetes-induced increase in leukocyte superoxide generation (leukocyte activation) is inhibited in leukocytes from iNOS^{-/-}→WT or PARP-1^{-/-}→WT chimeras. We conclude that diabetes is sufficient to activate both endothelial cells and leukocytes in the retina of WT and WT→WT mice but not in iNOS^{-/-}→WT or PARP-1^{-/-}→WT mice, and the result is that leukostasis is inhibited in the chimeras.

Additional mechanisms by which leukocytes might kill retinal endothelial cells include the FasL/Fas system and the release of reactive oxidant species. We provide evidence that these mechanisms do contribute to leukocyte-mediated

endothelial cell death in coculture, and these processes are inhibited when iNOS is absent from marrow-derived cells only.

Diabetes increased mRNA of proinflammatory molecules (TNF- α , iNOS, and ICAM-1) in the retina of WT mice, but not in the retina of iNOS^{-/-}→WT and PARP1^{-/-}→WT chimeras. These results, combined with the diabetes-induced increases in retinal superoxide, suggest that marrow-derived cells from diabetic animals induce inflammation in the neural retina without migrating out of the blood vessels into the neural retina. Nevertheless this inflammation did not cause a reduction in the number of ganglion cells in the neural retina. Although cocultures of mRECs incubated with leukocytes demonstrate that leukocytes from diabetic animals can kill endothelial cells and induce endothelial superoxide generation under those in vitro conditions, it is not clear in vivo if the toxic effects of leukocytes on endothelial cells are direct (i.e., Fas/FasL or transcellular delivery of toxic products such as superoxide) or indirect.

G-CSF controls maturation of myeloid precursor cells into granulocytes, notably neutrophils. Reduced susceptibility of the G-CSFR^{-/-} chimera to develop diabetes-induced vascular lesions of the retina provides strong evidence that neutrophils (and perhaps monocytes) play critical roles in development of the early stages of DR. Both neutrophils and monocytes adherent to the perfused retinal vasculature were observed in diabetic WT and GFP→WT mice. Monocyte function has been reported to be impaired in G-CSFR-deficient animals, thus leading to ambiguity about the role of cells in the monocyte lineage in the pathogenesis of retinopathy (49). The conclusion that neutrophils, and perhaps monocytes, damage the retinal vasculature in diabetes is further supported by in vitro studies in which the ability of leukocyte subtypes from diabetic animals to kill retinal endothelial cells was assessed. Interestingly, only a subset of neutrophils and monocytes show the diabetes-induced increase in iNOS expression, suggesting

that the vascular pathology might only be caused by a small fraction of these cells.

Marrow-derived cells apparently also contribute to the development of diabetes complications in other tissues. Microglia have been implicated in diabetes-induced allodynia in diabetic mice (20). We extend this by showing that deletion of either iNOS or PARP1 only from marrow-derived cells inhibits the development of this diabetes-induced tactile allodynia. Our evidence that the neural dysfunction is secondary to the activity of these enzymes in myeloid-derived cells has been previously unrecognized. It remains unclear if marrow-derived cells other than microglia are involved in diabetes-induced tactile allodynia.

Future investigations on the pathogenesis of diabetes complications need to expand beyond the traditional tissue- or vascular-specific view of complications to also include bone marrow-derived cells. It is not yet clear what activates the inflammatory-like processes in diabetes, but inflammatory processes in marrow-derived cells offer a new therapeutic target to inhibit the development of diabetes complications.

ACKNOWLEDGMENTS

This work was funded by the National Institutes of Health (EY-000300) and the Medical Research Service of the Department of Veterans Affairs. Support was also provided by Visual Science Research Training Grant 5T32EY007157 from the National Eye Institute (A.A.V.) and the CWRU Visual Science Research Center core facility (P30EY11373).

No potential conflicts of interest relevant to this article were reported.

G.L. researched data and wrote the manuscript. A.A.V. and R.R.T. researched data and wrote and edited the manuscript. X.W. and N.S. researched data. R.A.G.-K. reviewed the manuscript. T.S.K. wrote and edited the manuscript. T.S.K. is the guarantor of this work and, as such, had full access to all the data in the study and takes responsibility for the integrity of the data and the accuracy of the data analysis.

G-CSFR^{-/-} mice were kindly provided by Dr. D. Link (Washington University, St. Louis, MO). MCSF-R^{-/-} fetal liver cells were kindly provided by Dr. R. Stanley (Albert Einstein College, New York, NY). Nymph-R14 was kindly provided by Dr. E. Pearlman (Case Western Reserve University).

REFERENCES

- Davis MD, Kern TS, Rand LI. Diabetic retinopathy. In *International Textbook of Diabetes Mellitus*. 2nd ed. Alberti KGMM, Zimmet P, DeFronzo RA, Eds. New York, John Wiley & Sons, 1997, p. 1413–1446
- Barber AJ, Lieth E, Khin SA, Antonetti DA, Buchanan AG, Gardner TW. Neural apoptosis in the retina during experimental and human diabetes. Early onset and effect of insulin. *J Clin Invest* 1998;102:783–791
- Bresnick G, Engerman R, Davis MD, de Venecia G, Myers FL. Patterns of ischemia in diabetic retinopathy. *Trans Sect Ophthalmol Am Acad Ophthalmol Otolaryngol* 1976;81:694–709
- Kern TS. Contributions of inflammatory processes to the development of the early stages of diabetic retinopathy. *Exp Diabetes Res* 2007;2007:95103
- Zheng L, Szabó C, Kern TS. Poly(ADP-ribose) polymerase is involved in the development of diabetic retinopathy via regulation of nuclear factor-kappaB. *Diabetes* 2004;53:2960–2967
- Zheng L, Du Y, Miller C, et al. Critical role of inducible nitric oxide synthase in degeneration of retinal capillaries in mice with streptozotocin-induced diabetes. *Diabetologia* 2007;50:1987–1996
- MacMicking JD, Nathan C, Hom G, et al. Altered responses to bacterial infection and endotoxic shock in mice lacking inducible nitric oxide synthase. *Cell* 1995;81:641–650
- Altmeyer M, Barthel M, Eberhard M, Rehrauer H, Hardt WD, Hottiger MO. Absence of poly(ADP-ribose) polymerase 1 delays the onset of *Salmonella enterica* serovar *Typhimurium*-induced gut inflammation. *Infect Immun* 2010;78:3420–3431
- Kim SF, Huri DA, Snyder SH. Inducible nitric oxide synthase binds, S-nitrosylates, and activates cyclooxygenase-2. *Science* 2005;310:1966–1970
- Leal EC, Manivannan A, Hosoya K, et al. Inducible nitric oxide synthase isoform is a key mediator of leukostasis and blood-retinal barrier breakdown in diabetic retinopathy. *Invest Ophthalmol Vis Sci* 2007;48:5257–5265
- Zhao K, Huang Z, Lu H, Zhou J, Wei T. Induction of inducible nitric oxide synthase increases the production of reactive oxygen species in RAW264.7 macrophages. *Biosci Rep* 2010;30:233–241
- Hassa PO, Covic M, Hasan S, Imhof R, Hottiger MO. The enzymatic and DNA binding activity of PARP-1 are not required for NF-kappa B co-activator function. *J Biol Chem* 2001;276:45588–45597
- Zerfaoui M, Errami Y, Naura AS, et al. Poly(ADP-ribose) polymerase-1 is a determining factor in Crm1-mediated nuclear export and retention of p65 NF-kappa B upon TLR4 stimulation. *J Immunol* 2010;185:1894–1902
- Joussen AM, Murata T, Tsujikawa A, Kirchhof B, Bursell SE, Adamis AP. Leukocyte-mediated endothelial cell injury and death in the diabetic retina. *Am J Pathol* 2001;158:147–152
- Kim SY, Johnson MA, McLeod DS, Alexander T, Hansen BC, Lutty GA. Neutrophils are associated with capillary closure in spontaneously diabetic monkey retinas. *Diabetes* 2005;54:1534–1542
- Joussen AM, Poulaki V, Le ML, et al. A central role for inflammation in the pathogenesis of diabetic retinopathy. *FASEB J* 2004;18:1450–1452
- Otto M, Bak S, Bach FW, Jensen TS, Sindrup SH. Pain phenomena and possible mechanisms in patients with painful polyneuropathy. *Pain* 2003;101:187–192
- Obrosova IG, Xu W, Lyzogubov VV, et al. PARP inhibition or gene deficiency counteracts intraepidermal nerve fiber loss and neuropathic pain in advanced diabetic neuropathy. *Free Radic Biol Med* 2008;44:972–981
- Vareniuk I, Pavlov IA, Obrosova IG. Inducible nitric oxide synthase gene deficiency counteracts multiple manifestations of peripheral neuropathy in a streptozotocin-induced mouse model of diabetes. *Diabetologia* 2008;51:2126–2133
- Tsuda M, Ueno H, Kataoka A, Tozaki-Saitoh H, Inoue K. Activation of dorsal horn microglia contributes to diabetes-induced tactile allodynia via extracellular signal-regulated protein kinase signaling. *Glia* 2008;56:378–386
- Kern TS, Miller CM, Du Y, et al. Topical administration of nepafenac inhibits diabetes-induced retinal microvascular disease and underlying abnormalities of retinal metabolism and physiology. *Diabetes* 2007;56:373–379
- Zheng L, Howell SJ, Hatala DA, Huang K, Kern TS. Salicylate-based anti-inflammatory drugs inhibit the early lesion of diabetic retinopathy. *Diabetes* 2007;56:337–345
- Chan-Ling T. Glial, vascular, and neuronal cytolysis in whole-mounted cat retina. *Microsc Res Tech* 1997;36:1–16
- Su X, Sorenson CM, Sheibani N. Isolation and characterization of murine retinal endothelial cells. *Mol Vis* 2003;9:171–178
- Du Y, Miller CM, Kern TS. Hyperglycemia increases mitochondrial superoxide in retina and retinal cells. *Free Radic Biol Med* 2003;35:1491–1499
- Kern TS, Mohr S. Nonproliferative stages of diabetic retinopathy: animal models and pathogenesis. In *Retinal Vascular Disease*. Joussen A, Gardner TW, Kirchof B, Ryan SJ, Eds. Berlin, New York: Springer-Verlag, 2007
- Auffray C, Fogg DK, Narni-Mancinelli E, et al. CX3CR1+ CD115+ CD135+ common macrophage/DC precursors and the role of CX3CR1 in their response to inflammation. *J Exp Med* 2009;206:595–606
- Calcutt NA, Jorge MC, Yaksh TL, Chaplan SR. Tactile allodynia and formalin hyperalgesia in streptozotocin-diabetic rats: effects of insulin, aldose reductase inhibition and lidocaine. *Pain* 1996;68:293–299
- Berti-Mattera LN, Kern TS, Siegel RE, Nemet I, Mitchell R. Sulfasalazine blocks the development of tactile allodynia in diabetic rats. *Diabetes* 2008;57:2801–2808
- Engerman RL, Kern TS. Aldose reductase inhibition fails to prevent retinopathy in diabetic and galactosemic dogs. *Diabetes* 1993;42:820–825
- Addison DJ, Garner A, Ashton N. Degeneration of intramural pericytes in diabetic retinopathy. *BMJ* 1970;1:264–266
- Engerman RL, Kern TS. Retinopathy in animal models of diabetes. *Diabetes Metab Rev* 1995;11:109–120
- Tang J, Mohr S, Du YD, Kern TS. Non-uniform distribution of lesions and biochemical abnormalities within the retina of diabetic humans. *Curr Eye Res* 2003;27:7–13

34. Rota R, Chiavaroli C, Garay RP, Hannaert P. Reduction of retinal albumin leakage by the antioxidant calcium dobesilate in streptozotocin-diabetic rats. *Eur J Pharmacol* 2004;495:217–224
35. Gubitosi-Klug RA, Talahalli R, Du Y, Nadler JL, Kern TS. 5-Lipoxygenase, but not 12/15-lipoxygenase, contributes to degeneration of retinal capillaries in a mouse model of diabetic retinopathy. *Diabetes* 2008;57:1387–1393
36. Xu H, Chen M, Mayer EJ, Forrester JV, Dick AD. Turnover of resident retinal microglia in the normal adult mouse. *Glia* 2007;55:1189–1198
37. Joussen AM, Poulaki V, Mitsiades N, et al. Suppression of Fas-FasL-induced endothelial cell apoptosis prevents diabetic blood-retinal barrier breakdown in a model of streptozotocin-induced diabetes. *FASEB J* 2003;17:76–78
38. Lee HO, Ferguson TA. Biology of FasL. *Cytokine Growth Factor Rev* 2003;14:325–335
39. Lentsch AB, Ward PA. Regulation of inflammatory vascular damage. *J Pathol* 2000;190:343–348
40. Niedermeier M, Reich B, Rodriguez Gomez M, et al. CD4+ T cells control the differentiation of Gr1+ monocytes into fibrocytes. *Proc Natl Acad Sci USA* 2009;106:17892–17897
41. Liu F, Wu HY, Wesselschmidt R, Kornaga T, Link DC. Impaired production and increased apoptosis of neutrophils in granulocyte colony-stimulating factor receptor-deficient mice. *Immunity* 1996;5:491–501
42. Dai XM, Ryan GR, Hapel AJ, et al. Targeted disruption of the mouse colony-stimulating factor 1 receptor gene results in osteopetrosis, mononuclear phagocyte deficiency, increased primitive progenitor cell frequencies, and reproductive defects. *Blood* 2002;99:111–120
43. Calcutt NA. Experimental models of painful diabetic neuropathy. *J Neurol Sci* 2004;220:137–139
44. Virág L, Szabó C. The therapeutic potential of poly(ADP-ribose) polymerase inhibitors. *Pharmacol Rev* 2002;54:375–429
45. Tinker AC, Wallace AV. Selective inhibitors of inducible nitric oxide synthase: potential agents for the treatment of inflammatory diseases? *Curr Top Med Chem* 2006;6:77–92
46. Talahalli R, Zarini S, Sheibani N, Murphy RC, Gubitosi-Klug RA. Increased synthesis of leukotrienes in the mouse model of diabetic retinopathy. *Invest Ophthalmol Vis Sci* 2010;51:1699–1708
47. Kern TS, Du Y, Miller CM, Hatala DA, Levin LA. Overexpression of Bcl-2 in vascular endothelium inhibits the microvascular lesions of diabetic retinopathy. *Am J Pathol* 2010;176:2550–2558
48. Hickey MJ, Granger DN, Kubes P. Inducible nitric oxide synthase (iNOS) and regulation of leucocyte/endothelial cell interactions: studies in iNOS-deficient mice. *Acta Physiol Scand* 2001;173:119–126
49. Gregory AD, Capoccia BJ, Woloszynek JR, Link DC. Systemic levels of G-CSF and interleukin-6 determine the angiogenic potential of bone marrow resident monocytes. *J Leukoc Biol* 2010;88:123–131